

# Determining DfT Hardware by VHDL-AMS Fault Simulation for Biological Micro-Electronic Fluidic Arrays

H.G. Kerkhoff, X. Zhang

CADTES-TDT Group  
MESA+ Institute for Nanotechnology  
Enschede, the Netherlands  
*h.g.kerkhoff@utwente.nl*

H. Liu, A. Richardson

Centre for Microsystems Engineering  
Lancaster University  
Lancaster, United Kingdom

P. Nouet, F. Azais

Laboratoire d'Informatique, de Robotique et  
le Microélectronique de Montpellier  
(LIRRM)  
Montpellier, France

**Abstract**—The interest of microelectronic fluidic arrays for biomedical applications, like DNA determination, is rapidly increasing. In order to evaluate these systems in terms of required Design-for-Test structures, fault simulations in both fluidic and electronic domains are necessary. VHDL-AMS can be used successfully in this case. This paper shows a highly testable architecture of a DNA Bio-Sensing array, its basic sensing concept, fluidic modeling and sensitivity analysis. The overall VHDL-AMS fault simulation of the system is shown.

## I. INTRODUCTION

In the context of the European FP6 Network of Excellence “PATENT”, the (fault) modeling of fluidic components and the testing of fluidic bio-MEMS arrays by introducing Design-for-Test (DfT) structures is being investigated. To avoid the difficult testing of passive fluidic MEMS parts, e.g. the valves in a thermal-mechanical pump, the FlowFET [1] has been introduced as new fluidic transport device. It uses insulated gate electrodes on top of a fluidic channel, which causes a (bi-directional) fluidic flow, depending on the polarity of a high voltage being applied.

Testing of bio-sensing (disposable) arrays will be of crucial importance in terms of costs, quality and reliability. The capability of efficient structural test generation for detecting actual defects requires knowledge on anticipated defects, fault modeling and fault simulation, as well as insight where to insert Design-for-Test structures to enable controllability and observability. This means that the fault simulation of the entire multi-domain system is required under realistic defects to be expected in the fluidics as well as electrical domain. VHDL-AMS provides the possibilities to perform multi-domain fault simulations. Fluidic simulations [2] have formed the basis to derive the pressure distribution versus gate electrode under many conditions of the FlowFET. This data has been used to perform VHDL-AMS array simulations, based on the FlowFET and fluidic

crossovers. Beside fluidic behaviour, also the electronic behavior of all control and signal processing electronics has to be modeled and integrated in the overall electronic system behaviour. Co-simulation of electronic and fluidic domain VHDL-AMS fault simulations provide the designer useful information on how to detect/test anticipated defects in the multi-domain system, and also guidance to the proper location for DfT structures.

This paper is organized as follows: first the overall oscillator-based architecture of the DNA micro-electronic fluidic (MEF) bio-array is treated. Next, the DNA sensing principle is explained, and sensor and fluidic modeling elucidated. Subsequently the sensitivity of our oscillator approach is evaluated. Finally, the overall VHDL-AMS simulation is presented of the DNA MEF array and the effects of faults shown.

## II. ARCHITECTURE OF DNA BIO-SENSING MEF ARRAY

In recent years, much research has started up in electronically-based arrays for DNA detection, like e.g. [3]. One of the interesting approaches in that area makes use of DNA hybridization principles [4, 5]. Basically, a capacitor will change its value under the influence of DNA hybridization in a fluid if one side is covered with a label DNA.

Fig. 1 shows the set-up of our capacitive DNA MEF array [6] based on the DNA hybridization principle. The fluidic flow is electronically controlled using FlowFETs [1]. The FlowFETs and hence fluidic flow is controlled by a microcontroller. The different capacitors with different label DNA on one side of the electrode are subsequently scanned by means of a multiplexer circuit. Each capacitor is then shortly connected to a single oscillator, which will start

oscillating at a frequency determined by the capacitor. The number of transitions is counted during a time  $T_{obs}$ , and the resulting digital word is stored in a register. Obviously, this word is a measure for the degree of DNA hybridization of this particular capacitor. Each capacitor in the array will hence provide a unique word in this register. The actual construction has been discussed in [6].

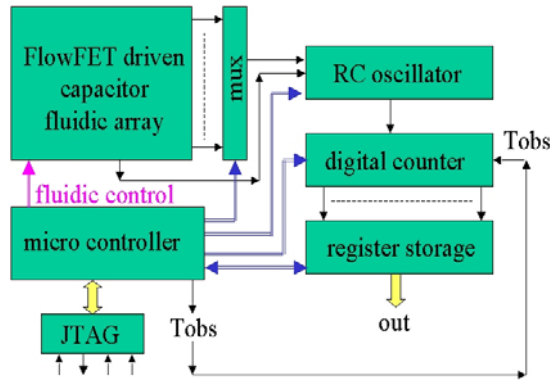


Figure 1. Basic scheme of the DNA capacitive sensor array including signal-processing part.

The combination of digital words provides data for recognition of the DNA sample. Special care has been paid with regard to testing this architecture, via the IEEE 1149.1 standard (JTAG) port. The controller, digital counter and registers are tested using standard digital scan techniques. The oscillator can be tested using reference oscillations. Fluidic flow in the array can be monitored electronically by means (control-voltage level and addressing time) which have been previously described [7]. In the next sections, the DNA hybridization (FlowFET driven capacitor fluidic array, Fig.1) and fluidic modeling are subsequently treated.

### III. SENSING ELEMENT MODEL

In this section, an equivalent electrical RC circuit model for a sensing element is developed, which could be used to assess the impact of fault and degradation mechanisms. The sensing element is composed of two bare planar rare-metal electrodes in an electrolyte solution. The properties on the electrode/electrolyte interface are of importance because the sensing mechanism is to detect the variations of the interface capacitance and some degradation concerned with the interface properties, as such as bio-fouling or holes. An electrical double layer (EDL), which is composed of the compact layer and the diffusion layer, forms spontaneously near the electrode surface in the electrolyte. The total impedance  $Z_T$  including the EDL and bulk solution is represented as a parallel RC circuit.  $R$  and  $C$  are dependent upon the applied potential frequency and electrolyte conductivity. At high frequencies,  $Z_T$  is dominated by bulk solution and the EDL impedance is negligible.  $C$  tends to be a constant value of a parallel plate capacitor with the permittivity of bulk electrolyte;  $R$  is also a constant value

that is inversely proportional to the conductivity. At low frequencies, the EDL effect is included in  $Z_T$ . Therefore, the signal frequencies in the sensing element must be in low range to extract the EDL properties, normally lower than 100Hz.

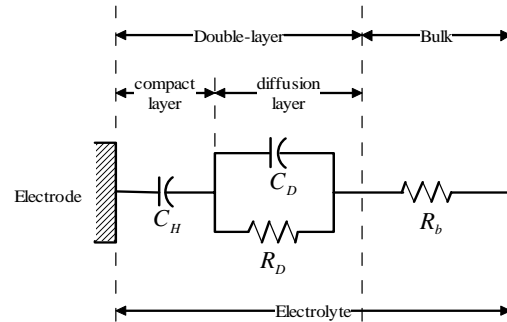


Figure 2. Equivalent electrical model for the electrode/electrolyte.

A RC circuit model is shown in Fig. 2.  $C_H$  and  $C_D$  are the capacitance of the compact-layer and the diffusion-layer respectively;  $R_D$  and  $R_b$  are the diffusion-layer resistance and the bulk resistance. There is no resistance effect in the compact-layer because the ions in this layer are to a first approximation immobilized. The effect of DNA hybridization and surface degradation could be easily expressed in this model and detected by for example oscillation-based testing (OBT). The effectiveness of this model for DNA hybridization process is explained by referring to Fig. 3. In the case of a bare electrode, the overall EDL capacitance is dominated by the diffusion-layer. However, after functionalization and immobilization of probe DNA onto the electrode, a bio-layer is formed on the electrode surface which mainly affects the dielectric constant and the length of the compact layer, while the dielectric constant and the length of the diffusion-layer are preserved.

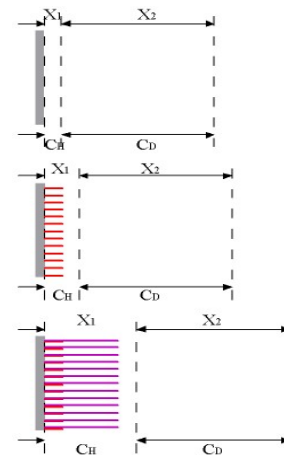


Figure 3. DNA Hybridization Process in EDL range.

Thus, the overall EDL capacitance is dominated by the compact-layer capacitance. Finally in the case of a hybridized electrode, an increase in both the layer thickness

and the dielectric constant is observed in the compact-layer. The decrease of the capacitance of the compact-layer resulting from DNA hybridization is very close to the decrease of the overall capacitance for every single sensing element and could be detected.

The previous model and experimental data was used for modeling the sensing part in VHDL-AMS. The equivalent values in permeability and oxide thickness are shown below in Fig. 4 for four regions subsequently: bare electrode, functionalization (label DNA), sample DNA hybridization and a failure.



Figure 4. VHDL-AMS simulation input ( $\epsilon_r$  and  $t_{ox}$ ) in the case of a bare Au electrode, functionalization, DNA hybridization and failure.

#### IV. FLOWFET FLUIDIC MODELING

In an implementation using fluidic channels, and the sensing part located in a “reactor” well, a controlled fluidic flow is preferred. This implementation takes into account the isolated electrodes of FlowFETs, and the direct contact electrodes of the sensing part. The latter can be put on the “drain” voltage of the FlowFETs.

Extensive fluidic (3D) FlowFET simulations have been carried out under fault-free as well as realistic faulty (e.g. oxide pin-hole) conditions [1, 2], after which VHDL-AMS (fault) models have been developed. This has not been done before in fluidics.

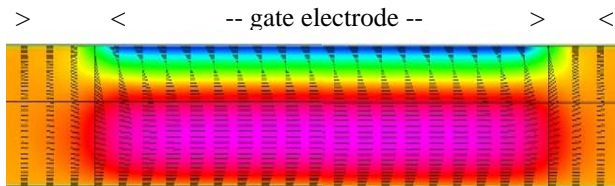


Figure 5. CFD-ACE 3-D velocity simulation of the FlowFET in longitudinal direction.

A fluidic velocity simulation in a section of a fluidic channel with on top an insulated electrode (FlowFET) is shown in Fig. 5. Based on the previous simulation data, a VHDL-AMS model was derived via fitting techniques for a FlowFET of rather the *pressure* versus gate voltage. It has

been further extended to VHDL-AMS simulations of a Micro-Electronic-Fluidic (MEF) array based on FlowFETs and cross-channels, in order to assist the designer in the proper choice of test signals and additional observation points to guarantee the quality. The simulation result is shown in Fig. 6, of a four by four array of FlowFETs. Two inputs are subsequently activated, and jointly dumped in a reaction well, resulting in the addition of fluids. Any problem in the FlowFETs (e.g. oxide breakdown) or fluidic channels (e.g. jamming, leakage) will immediately show up. The combination of straight-forward electronic VHDL-AMS descriptions (oscillator, registers etc.) and the sensing and fluidic VHDL-AMS descriptions, will enable the designer full (fault) simulation of this multi-domain system.

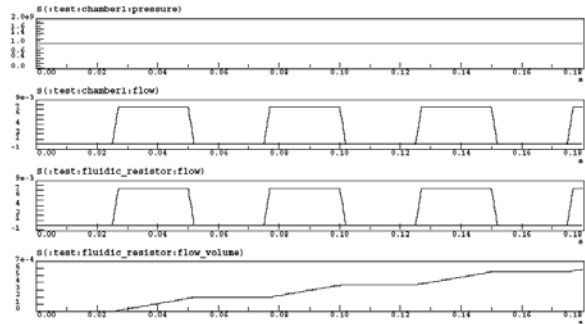


Figure 6. VHDL-AMS simulation result of a fluidic transport array (4 x 4), including pressures involved and flow. The last graph shows the accumulation of fluid in a reactor well.

In the next section, we will elucidate on the sensitivity of the oscillator with regard to the expected capacitive variations due to hybridization.

#### V. OSCILLATOR DESIGN

A sensitive and reliable oscillator is a key component for the bio-sensing array system. There exist many types of oscillators such as crystal oscillators, LC oscillators, RC oscillators etc. However, one important feature for our system is the possibility to realize the oscillator in a CMOS technology. Consequently, we have chosen to look for simple RC oscillators. In particular, two potential architectures have been investigated depending whether only *one* or *both* the electrodes of the capacitive sensor can be accessed. It turns out that both (RC relaxation and Schmitt-trigger based) result in similar behavior.

The first architecture is a very simple CMOS relaxation oscillator that uses both the electrodes of the sensor. As illustrated in Fig. 7, it makes use of two inverters together with an RC network. This architecture has been chosen because it is extremely simple to integrate. It provides a digital signal at a frequency equal to:

$$f_{osc} = \frac{1}{2.2 RC} \quad (1)$$

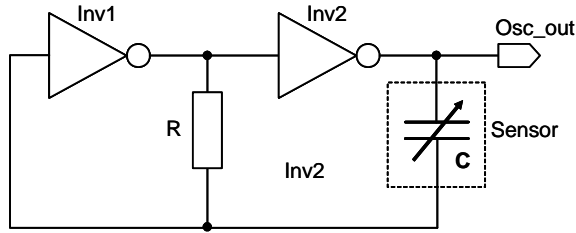


Figure 7. CMOS relaxation oscillator.

For a given value of the sensor capacitance, the nominal oscillation frequency can then be easily adjusted in the desired range by choosing an appropriate value for the resistance of the RC network. Fig. 8 gives a transient simulation result for an oscillator using the following design parameters:  $R=10\text{k}\Omega$ ,  $C=1\text{nF}$  (nominal value). Both inverters are standard cells taken from a foundry design library:  $L=0.8\mu\text{m}$ ,  $W_p=36\mu\text{m}$  and  $W_n=20\mu\text{m}$ .

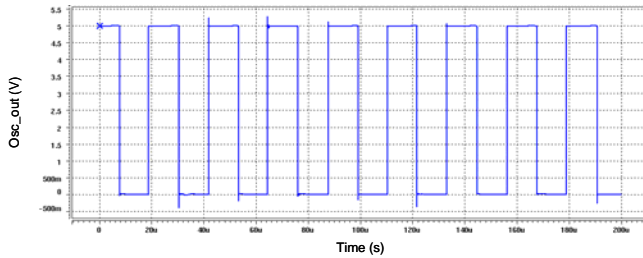


Figure 8. Transient simulation of the CMOS relaxation oscillator

This oscillator provides a digital signal at a frequency of about 45 kHz. In Fig. 9, a parametric analysis is given to study the response of the oscillator frequency as a function of the sensor capacitance variation. It is observed that an increase in the oscillator frequency results if the sensor capacitance decreases. Considering a nominal value of 1nF for the sensor capacitance in case of bare gold electrodes and a deviation of about 50% after DNA hybridization, the oscillation frequency is increased from 45 kHz up to 85 kHz. This frequency variation is sufficient to be processed by standard electronics. In case of a faulty device, we expect to have a much lower value for the sensor capacitance, which will result in a much higher oscillation frequency. Note that due to the  $1/C$  dependency of the oscillation frequency, one can expect a very good sensitivity with respect to failure mechanisms producing a decrease of the sensor capacitance.

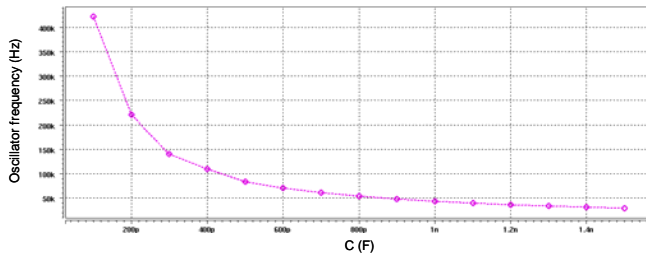


Figure 9. Oscillator frequency as a function of the sensor capacitance.

The second architecture we have investigated is a classical relaxation oscillator based on a Schmitt trigger configuration. This architecture presented in Fig. 10 uses only one electrode on the sensor. It combines an RC network with an opamp Schmitt trigger circuit. It delivers a square-wave signal at a frequency equal to:

$$f_{osc} = \frac{1}{2 RC \ln\left(1 + 2 \frac{R1}{R2}\right)} \quad (2)$$

Similarly to the previous architecture, the nominal oscillation frequency can be adjusted in the desired frequency range by choosing appropriate values for the resistances, considering a given value of the sensor capacitance.

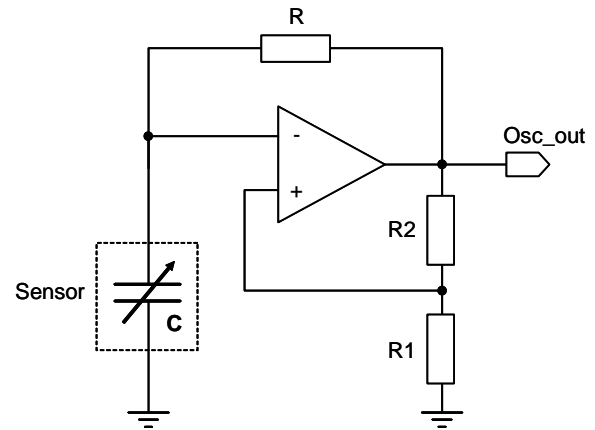


Figure 10. Schmitt trigger relaxation oscillator.

Figure 11 gives the transient simulation result of the oscillator with the following design parameters:  $R=R1=R2=10\text{k}\Omega$ ,  $C=1\text{nF}$  (nominal value). The opamp is a classical opamp obtained from the foundry design library.

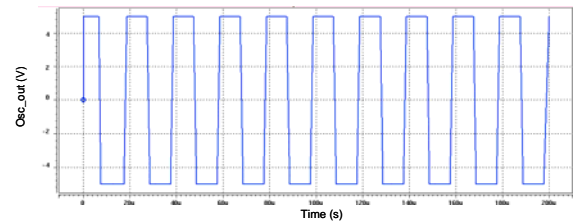


Figure 11. Transient simulation of the Schmitt trigger relaxation oscillator.

The parametric analysis to study the response of the oscillator frequency as a function of the sensor capacitance variation leads to similar results as with the previous architecture.

## VI. VHDL-AMS SIMULATION OF MEF DNA ARRAY

Also the electronic part of the capacitive DNA MEF array was completely modeled and fault simulated using VHDL-AMS providing full insight in the entire fluidic-electronic system to the designer. The control signals and results, based on previous data and modeling are given in Fig. 12. Co-simulation of electronic and fluidic domain VHDL-AMS fault simulations provide the designer information on how to detect/test anticipated defects in the multi-domain system. The last signal shows the oscillator response under the four conditions of bare electrode, functionalization, hybridization and a defect.



Figure 12. VHDL-AMS simulation result of the oscillation-based DNA sensor array. The last signal shows the oscillation frequency in the previous situations (Fig. 4).

## VII. CONCLUSIONS

A highly testable architecture of a DNA bio-sensing MEF array has been presented. The front-end capacitive sensing modeling has been discussed, as well as the FlowFET-based fluidic modeling. The detection sensitivity by means of an oscillation-based technique has been treated. Overall VHDL-AMS fault simulation has been used to evaluate the architecture with respect to its sensitivity to detect faults.

## REFERENCES

- [1] H.G. Kerkhoff, R. Barber, D. Emerson, R. Muller, O. Nedelcu, and E. van der Wouden, "Design and Test of Micro-Electronic Fluidic Systems", DATE Workshop on MEMS/MST, Munich, pp. 47 - 52, March 2005.
- [2] H.G. Kerkhoff, R. Barber, X. Zhang and D. Emerson, "Fault Modelling and Co-Simulation in FlowFET-Based Biological Array Systems", accepted for DELTA06, Kuala Lumpur, Malaysia, January 2006.
- [3] Roland Thewes, Franz Hofman, and etc., "Sensor Arrays for Fully-Electronic DNA Detection on CMOS", ISSCC 2002/ SESSION 21/ TD: SENSORS AND MICROSYSTEMS/ 21.2
- [4] Christine Berggren et al., "A Feasibility Study of a Capacitive Biosensor for Direct Detection of DNA Hybridization", Electroanalysis 1999, Vol. 11, No. 3, pp. 156-160.

- [5] C. Guiducci, C. Stagni, B. Ricco et al., "DNA detection by integrable electronics", Biosensors and Bioelectronics 19, pp. 781-787, 2004.
- [6] H. Li, H.G. Kerkhoff, A. Richardson, X. Zhang, P. Nouet and F. Azais, "Design and Test of an Oscillation Based System Architecture for DNA Sensor Arrays", 11<sup>th</sup> IEEE International Mixed-Signals Testing Workshop, Cannes, France, pp. 234-239, June 2005.
- [7] H.G. Kerkhoff and M. Acar, "Testable Design and Testing of Micro-Electro-Fluidic Arrays", in Proc. VLSI Testing Symposium (VTS), ISBN 0-7695-1924-5, Nappa, USA, April 2003, pp. 12A:1-7.